GEOPHYSICAL RESEARCH LETTERS, VOL. 35, L10809, doi:10.1029/2007GL032628, 2008

Timescale analysis of aerosol sensitivity during homogeneous freezing and implications for upper tropospheric water vapor budgets

Jennifer E. Kay[1] and Robert Wood[2]

Received 13 November 2007; revised 18 February 2008; accepted 17 April 2008; published 23 May 2008.

[1] Using timescales for the generation and depletion of water vapor, we predict aerosol sensitivity in clouds formed by homogeneous freezing. Our timescale analysis explains why aerosol sensitivity increases dramatically with ice deposition coefficients (α_i) $\ll 0.1$, and also why aerosol sensitivity increases as vertical velocity increases, temperature decreases, aerosol number decreases, and aerosol size decreases. We combine existing in-situ observations with adiabatic parcel modeling to constrain $\alpha_i \geq 0.1$ for small ice crystals forming at high ice supersaturations. Two important implications for understanding and modeling upper tropospheric water vapor budgets emerge from our results: 1) aerosol sensitivity can be appreciable at low temperatures and moderate updrafts ($\sim$5 cm/s) in the upper tropical troposphere, 2) reconciling our results with recent laboratory measurements supports theory that α_i increases with ice supersaturation and/or decreases with ice crystal size. **Citation:** Kay, J. E., and R. Wood (2008), Timescale analysis of aerosol sensitivity during homogeneous freezing and implications for upper tropospheric water vapor budgets, *Geophys. Res. Lett.*, *35*, L10809, doi:10.1029/2007GL032628.

1. Introduction

[2] The sensitivity of clouds to aerosol properties is an important area of climate research. *Twomey* [1974] described the first indirect effect of increasing aerosol concentrations (N_a [m^{-3}]) on clouds: For a fixed water content, the drop number concentration and brightness of warm clouds increases.

[3] In contrast, modeling studies have shown that the number of ice crystals (N_i [m^{-3}]) resulting from homogeneous freezing is relatively insensitive to upper tropospheric N_a [e.g., *Jensen and Toon*, 1994; *DeMott et al.*, 1997; *Kärcher and Lohmann*, 2002a, 2002b; *Kärcher and Ström*, 2003]. In other words, these studies imply weak aerosol sensitivity, or that increasing N_a has a negligible effect on N_i or $\eta_a \ll 1$ where η_a is an aerosol sensitivity parameter defined as:

$$\eta_a \equiv \frac{d(\ln\ N_i)}{d\ \ln(N_a)} \tag{1}$$

Observations show a positive but weak correlation between N_i and N_a during cold cloud formation [*Seifert et al.*, 2004]. If η_a is larger than these studies suggest, an increase in anthropogenic N_a will increase cold cloud N_i. For a fixed water content, increasing N_i will increase cold cloud albedos and alter radiative fluxes. In addition, increasing N_i will increase the drawdown of supersaturation in the upper tropical troposphere and therefore alter the water vapor budget of the stratosphere. Given the influence of cold cloud microphysical properties on radiative fluxes and water vapor budgets, it is important to understand the atmospheric conditions under which cold clouds are sensitive to changes in N_a.

[4] In this paper, we investigate the physical factors that determine η_a in cold clouds formed by homogeneous freezing. Although aerosols that serve as heterogeneous ice nuclei can alter cold cloud properties, we do not consider the impact of heterogeneous freezing on cold cloud aerosol indirect effects. Heterogeneous freezing is not well constrained by observations or theory. In addition, observations of large ice supersaturations [e.g., *Ovarlez et al.*, 2002; *Jensen et al.*, 2001] and low ice nuclei concentrations [e.g., *DeMott et al.*, 2003] suggest that homogeneous freezing of aqueous aerosols is an important ice formation mechanism in the upper troposphere. In Section 2, we use an adiabatic parcel model with binned ice microphysics [*Kay et al.*, 2006] to demonstrate that a simple timescale ratio explains the dependence of η_a upon thermodynamic factors including vertical velocity (w [m s^{-1}]) and co-varying temperature (T [°C]) and pressure (P [mb]), and microphysical factors including N_a, dry aerosol radius ($r_{a\text{-}dry}$ [m]), and the ice deposition coefficient or mass accommodation coefficient (α_i). In Section 3, we discuss the implications of our results for the atmosphere. In Section 4, we summarize our results and provide suggestions for future work.

[5] Our work builds on the analytical results of *Kärcher and Lohmann* [2002a, 2002b] (hereafter KL). KL found that N_i is primarily controlled thermodynamically rather than microphysically, with a strong dependence upon w. KL compared ice crystal growth timescales to the timescale of the freezing event, and found two homogeneous freezing regimes: a "fast-growth" and a "slow-growth" regime. Yet, KL did not consider two important microphysical factors: 1) KL did not address the current uncertainty in α_i, i.e., the fraction of impinging water vapor molecules that are incorporated into an ice crystal lattice [*Pruppacher and Klett*, 1997]. KL assumed $\alpha_i = 0.5$ in their analysis, but laboratory measurements of α_i vary from 0.006 to 1 [e.g., *Haynes et al.*, 1992; *Magee et al.*, 2006]. 2) KL did

[1] Climate and Global Dynamics, National Center for Atmospheric Research, Boulder, Colorado, USA.
[2] Department of Atmospheric Sciences, University of Washington, Seattle, Washington, USA.

0094-8276/08/2007GL032628$05.00

not explicitly treat the depletion of N_a by freezing, a crucial factor when N_i are limited by N_a.

2. What Determines η_a?

[6] For simplicity, we consider cold cloud formation during adiabatic ascent at constant w. The supersaturation with respect to ice (S_i) increases during ascent and, at the beginning of freezing (time t = 0), the homogeneous freezing rate (J_{hom} [m^{-3} s^{-1}]), an exponentially increasing function of S_i reaches a threshold value (J_o [m^{-3} s^{-1}]). Freezing stops at a later time (t_{event} [s]) when vapor deposition on newly formed ice crystals causes S_i to decrease and J_{hom} to decrease below J_o. Given this physical picture of cloud formation, the N_i generated in a homogeneous freezing event can be approximated as:

$$N_i = \int_0^{t_{event}} J_{hom}(S_i(t)) \frac{4}{3} \pi r_a(t)^3 N_a(t) dt \tag{2}$$

With this physical model of cold cloud formation, the partitioning of water between the ice and vapor phase depends on a competition between lifting (cooling), which increases S_i, and ice crystal growth, which depletes S_i. Using timescale notation, the dependence of S_i on the competition between lifting and growth can be expressed as:

$$\frac{dS_i}{dt} = \frac{S_i}{\tau_{lift}} - \frac{S_i}{\tau_{growth}} \tag{3a}$$

where τ_{lift} is the timescale for increase of S_i via cooling through ascent, and τ_{growth} is a timescale for growth of freshly- nucleated ice crystals by vapor deposition. Because ice crystal growth results from vapor deposition, τ_{growth} is also a timescale for the drawdown of S_i.

[7] We hypothesize that η_a can be predicted by the timescale ratio, R.

$$R \equiv \frac{\tau_{growth}}{\tau_{lift}} \tag{3b}$$

In other words, η_a is entirely determined by the competition between the rates of lifting (cooling) and ice crystal growth. When $R \gg 1$ ice crystal growth is relatively slow when compared with the cooling that increases S_i. Consequently, large S_i values occur for long periods, and almost all of the available aerosol can freeze (η_a approaches 1). When $R \ll 1$, ice crystal growth is relatively fast when compared to cooling. As a result, large S_i are quickly reduced, and only a small number of the available aerosol can freeze (η_a approaches 0). Note that $R \gg 1$ is roughly equivalent to KL's "fast growth" regime while $R \ll 1$ is roughly equivalent to KL's "slow growth regime".

[8] To evaluate if R can quantitatively predict the aerosol sensitivity parameter η_a, analytical expressions for τ_{lift} and τ_{growth} are required. In an analytical analysis of a rising adiabatic parcel based on equation (2) and KL, the time constants τ_{lift} and τ_{growth} arise naturally and are defined as follows:

Table 1. Parcel Model Description and Configuration Used in This Study[a]

	Details
Description	description and validation from *Kay et al.* [2006]
	binned ice microphysics (300 bins)
	monodisperse sulfuric acid aerosol with an individual dry weight of 10^{-16} kg and variable number concentration (N_a)
	saturation vapor pressures e_s and es_{ice} from *Murphy and Koop* [2005]
Configuration	parcel lifted at a constant vertical velocity (w)
	homogeneous freezing [*Koop et al.*, 2000] only
	ice crystal fallout included with parcel depth = 100 m

[a]In all model runs, α_i does not depend on ice crystal size or on ice supersaturation. Using a monodisperse size distribution accentuates aerosol sensitivity for model runs with $\alpha_i < 1$.

$$\tau_{lift} = [Q_1 w]^{-1} \tag{4}$$

with

$$Q_i = \frac{\Gamma}{T}\left(\left(\frac{L_s(S_i+1)}{R_v T}\right) - \frac{5}{2}\right)$$

where Q_1 is a thermodynamic constant, $\Gamma = 0.0098$ K m^{-1} is the dry adiabatic lapse rate (appropriate for the low temperatures being considered), $L_s = 2.834 \times 10^6$ J kg^{-1} is the latent heat of sublimation, and $R_v = 461$ J K^{-1} kg^{-1} is the gas constant for water vapor.

$$\tau_{growth} = \left[(KN_a)^{2/3}\left(S_i D_v^*\right)\right]^{-1} \tag{5}$$

with

$$K = \sqrt{2(\rho_{sat-i}\rho_i)}$$

and

$$D_v^* = \frac{D_v}{\frac{r_a}{r_a+\lambda} + \frac{D_v}{r_a \alpha_i}\sqrt{\frac{2\pi M_w}{R_{ideal} T}}} = \frac{D_v}{\frac{r_a}{r_a+\lambda} + \frac{\lambda}{\alpha_i r_a}}$$

where K is a constant, $\rho_{\text{sat-i}}$ is the saturation vapor density with respect to ice (kg m^{-3}), $\rho_i = 900$ kg m^{-3} is the density of ice, D_v^* is the modified vapor diffusivity (m^2 s^{-1}) [*Pruppacher and Klett*, 1997, equation (13-14)] which includes impedances to growth due to vapor diffusivity and surface processes but neglects the relatively small thermal impedance to growth, D_v is the vapor diffusivity (m^2 s^{-1}) [*Pruppacher and Klett*, 1997, equation (13-3)], λ is the molecular mean free path (m) [*Jacobson*, 1999, equation (16.20)], $M_w = 0.018015$ kg $mole^{-1}$ is the molecular weight of water, and $R_{\text{ideal}} = 8.3145$ J $K^{-1}mole^{-1}$ is the ideal gas constant.

[9] By calculating τ_{lift} and τ_{growth} in a number of model experiments (adiabatic parcel model with binned microphysics, configuration described in Table 1), we evaluate if

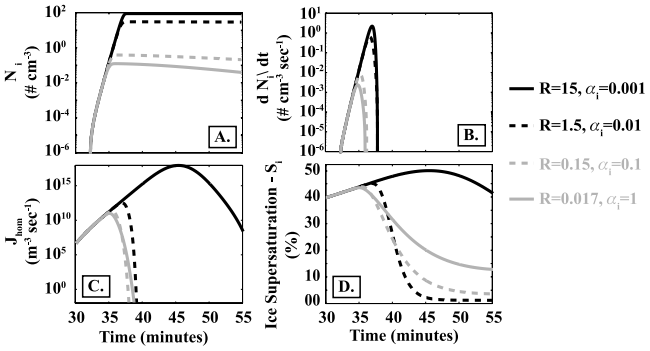

Figure 1. Time series of parcel model lifting experiments (Table 1) with w = 10 cm s^{-1}, T_0 = −50 C, P_0 = 250 mb, N_a = 100 cm^{-3}, and $r_{a\text{-}dry}$ = 0.2 μm.

η_a can be predicted by R alone. In all cases, we calculated R using the parcel model output at the time step before freezing begins, herein defined as when the ice particle production rate (dN_i/dt) exceeds 1 m^{-3} s^{-1}.

[10] To introduce our parcel model experiments, we first show an experiment in which we only vary α_i (Figure 1). Decreasing α_i increases R by increasing τ_{growth} without affecting τ_{lift}. Indeed, the increase in S_i and J_{hom} resulting from long τ_{growth} is why small α_i lead to large N_i [*Gierens et al.*, 2003]. The α_i lifting experiment reveals the dramatic effect of R on the sensitivity of N_i to N_a and on the drawdown of S_i. When efficient growth is assumed ($R \ll 1$, $\alpha_i > 0.1$, gray curves Figure 1), J_{hom} and S_i are quickly reduced by ice crystal growth, and N_i is not sensitive to N_a. In contrast, with inefficient growth ($\alpha_i \ll 0.1$, $R \gg 1$, black curves Figure 1), J_{hom} and S_i reach large values and the sensitivity of N_i to N_a increases. It is interesting to note that only the lowest α_i (α_i = 0.001) result in persistent high S_i (S_i > 40%) after the freezing event ends. Surprisingly, S_i is depleted faster when α_i = 0.01 than when α_i = 1. This counter-intuitive result is explained as follows: When α_i decreases, individual particles grow inefficiently allowing both the peak S_i and J_{hom} to increase. When the peak J_{hom} increases, N_i and the total surface area dramatically increase. Thus, even though individual particles are growing inefficiently, the increase in total ice surface area allows the S_i drawdown to be faster when α_i = 0.01 than when α_i = 1.

[11] Although the α_i lifting experiment revealed that there are complex relationships between η_a and atmospheric variables, our parcel model runs suggest that the aerosol sensitivity parameter η_a can be predicted by R alone (Figure 2a). When multiple parcel model experiments are plotted on one R versus η_a graph (Figure 2a), they collapse onto a single curve. In other words, one can predict changes in η_a by evaluating the effect of changing external atmospheric conditions on R (equation (3)).

[12] Using a sensitivity test approach, we explored the influence of plausible variations in thermodynamic (w, T, P) and microphysical (α_i, $r_{a\text{-}dry}$) variables on η_a and R (Figures 2b–2d). Through R, we can understand the physical basis for the influence of these parameters on η_a. Aerosol sensitivity increases with w through τ_{lift}. With $\alpha_i > 0.1$, η_a is small; however when $\alpha_i < 0.1$, τ_{growth} increases and η_a increases dramatically Aerosol sensitivity increases when $T \ll -70$°C because low T increases τ_{growth}. Finally, variations in $r_{a\text{-}dry}$ have only a limited influence on η_a. As $r_{a\text{-}dry}$ decreases, η_a slightly increases because for a fixed N_a, reducing $r_{a\text{-}dry}$ increases τ_{growth}.

3. Implications for the Atmosphere

[13] When $\alpha_i < 0.1$, plausible variations in α_i can dramatically change η_a, and alter the sensitivity of η_a to variations in other microphysical and thermodynamic variables. The influence of α_i on τ_{growth} is more important at

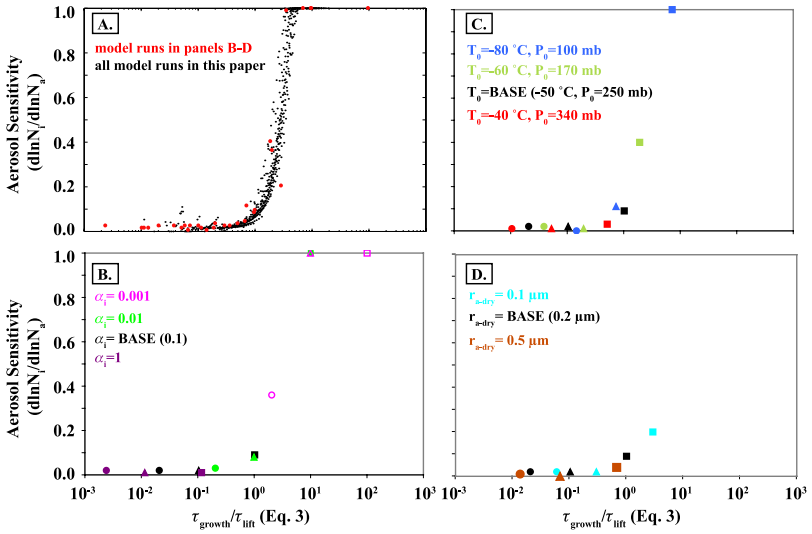

Figure 2. Aerosol sensitivity parameter (η_a) versus timescale ratio R for (a) all parcel model runs, and for (b–d) parcel model sensitivity tests with a range of α_i, T_0, and $r_{a\text{-}dry}$. Aerosol sensitivity (equation (1)) was calculated using the change in N_i from model runs with N_a = 100 cm^{-3} and N_a = 500 cm^{-3}. For Figures 2b–d, circles w = 2 cm s^{-1}, diamonds w = 10 cm s^{-1}, and squares w = 100 cm s^{-1}. Also for Figures 2b–d, base values were used unless otherwise indicated: T_0 = −50°C, P_0 = 250 mb, and $r_{a\text{-}dry}$ = 0.2 μm.

Table 2. INCA Observations and Parcel Model Predicted Ni[a]

	INCA Observations [*Kärcher and Ström*, 2003]					Parcel Model N_i (cm^{-3})			
	w ($cm\ s^{-1}$)	T (°C)	P (mb)	N_a (cm^{-3})	N_i (cm^{-3})	$\alpha_i = 1$	$\alpha_i = 0.1$	$\alpha_i = 0.01$	$\alpha_i = 0.006$
Scotland	26.2	−48.3	290	300	5.3	0.5	2.3	102.8	212.6
Chile	23	−46.8	275	110	1.1	0.4	1.4	61.3	102.7

[a]Parcel model N_i are found from constant lifting experiments (Table 1) with INCA-observed w, T, and N_a, and P_0. α_i values of 0.057 and 0.13 were required to match the mean Scotland and Chile observations, respectively.

low α_i because D_v^* does not depend directly on α_i, but on $r_a/(r_a + \lambda) + \lambda/\alpha_i r_a \approx 1 + \lambda/\alpha_i r_a$ (see equation (5)). When $\lambda/\alpha_i r_a \ll 1$, the precise value of α_i is unimportant because diffusive impediments to growth are more important than surface impediments to growth. Reviews of laboratory measurements at cold cloud temperatures suggest that α_i for ice crystals could be as low as 0.001 and as high as 1 [*Haynes et al.*, 1992]; recent laboratory measurements found $\alpha_i = 0.006$ [*Magee et al.*, 2006]. Given the sensitivity of η_a to α_i when $\alpha_i < 0.1$, discrepancies between α_i measurements must be resolved.

[14] Fortunately, existing observations can be used to constrain α_i for small ice crystals forming at high S_i in the atmosphere. In general, observed N_i (0.001–10 cm^{-3} [e.g., *Mace et al.*, 2001; *Kärcher and Ström*, 2003]) rarely approach observed N_a (10–500 cm^{-3} [e.g., *Rogers et al.*, 1998; *Minikin et al.*, 2003]). The INCA field campaign [*Kärcher and Ström*, 2003] provides a unique opportunity to constrain α_i. Using INCA measurements, we require $\alpha_i \approx 0.1$ to simultaneously match the mean N_i, N_a, T, and w in lifting parcel model experiments (Table 2). With $\alpha_i = 0.006$ [*Magee et al.*, 2006], modeled N_i are orders of magnitude larger than INCA-observed N_i. When present, shattering of ice crystals by aircraft probes [e.g., *Field et. al.*, 2003; *McFarquhar et al.*, 2007] and "aging" of ice crystal size distributions (e.g., via dispersion) would reduce observed N_i and increase the value of α_i required to match INCA observations with parcel modeling experiments. Indeed, matching modeled and observed N_i during a wave cloud case from SUCCESS suggests $\alpha_i > 0.5$ [*Jensen et al.*, 1998]. Uncertainty in the INCA-observed w also has an important effect on the constrained α_i. If a large range of w are considered (3 cm/s < w < 50 cm/s), a much larger range of α_i ($0.01 < \alpha_i < 1$) are consistent with the mean observed N_i.

[15] In summary, atmospheric observations suggest that η_a rarely approaches 1 and α_i are ≥ 0.1 for small ice crystals forming at high S_i. Therefore, laboratory observations of $\alpha_i = 0.006$ [*Magee et al.*, 2006], which were made at $S_i < 20\%$, may only be appropriate for large ice crystals or at low S_i. There is a theoretical basis for the latter possibility [*Nelson and Baker*, 1996], but further measurements are required to constrain the behavior of α_i as a function of S_i and ice crystal size.

[16] Assuming $\alpha_i = 0.1$ for small ice crystals forming at large S_i, cold clouds in the atmosphere primarily form in a regime where $\eta_a \ll 1$ (Figure 3). With $\alpha_i = 0.1$, our modeling results do suggest there are conditions under which N_i does depend on N_a. First, η_a increases at very large w (approximately $w > 100$ cm s^{-1} when $T = -50$°C and $\alpha_i = 0.1$). Second, there is a significant increase in η_a at low temperature. These results contrast with those of *Hoyle et al.* [2005], who suggested that T and P effects on τ_{growth} are in balance. Finally, η_a increases as N_a decreases, which can be important at high w or low T.

4. Summary and Discussion

[17] In this study, we used analytical analysis, parcel modeling, and observations to understand aerosol sensitivity during homogeneous freezing (η_a, equation (1)). We found the following.

[18] 1. The η_a can be explained and predicted using a single timescale ratio, R (equation (3)).

[19] 2. The η_a increases dramatically when $\alpha_i < 0.1$, but we constrain $\alpha_i \geq 0.1$ for small ice crystals forming at high S_i. With $\alpha_i = 0.1$, our model shows that η_a is small under most atmospheric conditions, but quickly increases to appreciable values with large w ($w > 100$ cm s^{-1} when T = −50°C) or at low T (w > 5 cm s^{-1} when $T = -80$°C).

[20] Simultaneous observations of N_a, N_i and w at low T could be used to estimate atmospheric α_i and to evaluate the dependence of η_a on T presented in this study. Observations of low N_i in the TTL [e.g., *Peter et al.*, 2003] may seem confounding to our modeling results, but could be consistent if homogeneous freezing occurs at very low w (e.g.,

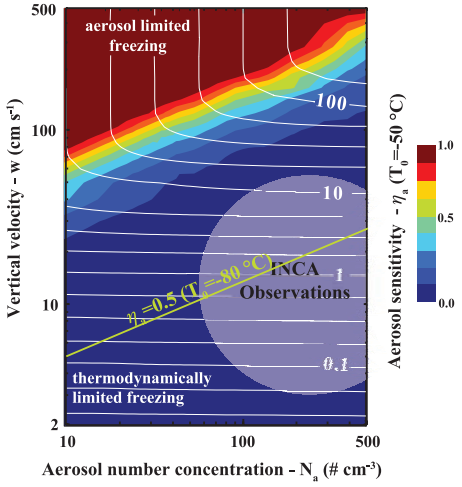

Figure 3. Maximum N_i contoured as a function of vertical velocity (w) and aerosol number concentration (N_a) from the parcel model lifting experiments with $\alpha_i = 0.1$, $T_0 = -50$°C, $P_0 = 250$ mb, and $r_{a\text{-}dry} = 0.2$ μm. Colors indicate the aerosol sensitivity parameter η_a (equation (1)) and range from the thermodynamically limited freezing regime ($\eta_a = 0$) to the aerosol-limited freezing regime ($\eta_a = 1$). The green line shows where $\eta_a = 0.5$ line for $T_0 = -80$°C and $P_0 = 100$ mb. The INCA field campaign observations are indicated in the transparent white circle (10–90% percentile values taken from *Kärcher and Ström* [2003] and *Minikin et al.* [2003]).

mm/s proposed by *Luo et al.* [2003]) or if measurements fail to detect small ice crystals. Finally, our work demonstrates the importance of constraining α_i variations as a function of S_i and ice crystal size. Understanding α_i variations will be especially important when evaluating if α_i can explain atmospheric observations of large persistent S_i in the upper troposphere [*Peter et al.*, 2006].

[21] **Acknowledgments.** J.E.K. was supported by NSF-ATM-02-1147. R.W. was supported by startup funds from the University of Washington. Both authors thank Dr. Marcia Baker for her encouragement and her contributions to this work.

References

DeMott, P. J., D. C. Rogers, and S. M. Kreidenweis (1997), The susceptibility of ice formation in upper tropospheric clouds to insoluble aerosol components, *J. Geophys. Res.*, *102*(D16), 19,575–19,584.

DeMott, P. J., D. J. Cziczo, A. J. Prenni, D. M. Murphy, S. M. Kreidenweis, D. S. Thomson, R. Borys, and D. C. Rogers (2003), Measurements of the concentration and composition of nuclei for cirrus formation, *Proc. Natl. Acad. Sci. U. S. A.*, *100*(25), 14,655–14,660.

Field, P. R., R. Wood, E. Hirst, R. Greenaway, P. Kaye, P. R. A. Brown, and J. A. J. Smith (2003), Ice particle interarrival times measured with a fast FSSP, *J. Atmos. Oceanic Technol.*, *20*, 249–261.

Gierens, K. M., M. Monier, and J. Gayet (2003), The deposition coefficient and its role for cirrus clouds, *J. Geophys. Res.*, *108*(D2), 4069, doi:10.1029/2001JD001558.

Haynes, D. R., N. J. Tro, and S. M. George (1992), Condensation and evaporation of H_20 on ice surfaces, *J. Phys. Chem.*, *96*, 8502–8509.

Hoyle, C. R., B. P. Luo, and T. Peter (2005), The origin of high ice crystal number densities in cirrus clouds, *J. Atmos. Sci.*, *62*(7), 2568–2579.

Jacobson, M. Z. (1999), *Fundamentals of Atmospheric Modeling*, 656 pp., Cambridge Univ. Press, New York.

Jensen, E. J., and O. B. Toon (1994), Ice freezing in the upper troposphere: Sensitivity to aerosol number density, temperature and cooling rate, *Geophys. Res. Lett.*, *21*(18), 2019–2022.

Jensen, E. J., et al. (1998), Ice Nucleation processes in upper tropospheric wave-clouds observed during SUCCESS, *Geophys. Res. Lett.*, *25*(9), 1363–1366.

Jensen, E., O. Toon, S. Vay, J. Ovarlez, R. May, T. Bui, C. Twohy, B. Gandrud, R. Pueschel, and U. Schumann (2001), Prevalence of ice-supersaturated regions in the upper troposphere: Implications for optically thin ice cloud formation, *J. Geophys. Res.*, *106*(D15), 17,253–17,266.

Kärcher, B., and U. Lohmann (2002a), A parameterization of cirrus cloud formation: Homogeneous freezing of supercooled aerosols, *J. Geophys. Res.*, *107*(D2), 4010, doi:10.1029/2001JD000470.

Kärcher, B., and U. Lohmann (2002b), A parameterization of cirrus cloud formation: Homogeneous freezing including effects of aerosols size, *J. Geophys. Res.*, *107*(D23), 4698, doi:10.1029/2001JD001429.

Kärcher, B., and J. Ström (2003), The roles of dynamical variability and aerosols in cirrus cloud formation, *Atmos. Chem. Phys.*, *3*, 823–838.

Kay, J. E., M. Baker, and D. Hegg (2006), Microphysical and dynamical controls on cirrus cloud optical depth distributions, *J. Geophys. Res.*, *111*, D24205, doi:10.1029/2005JD006916.

Koop, T., B. Luo, A. Tslas, and T. Peter (2000), Water activity as the determinant for homogeneous ice nucleation in aqueous solutions, *Nature*, *406*, 611–614.

Luo, B. P., et al. (2003), Ultrathin Tropical Tropopause Clouds (UTTCs): II. Stabilization mechanisms, *Atmos. Chem. Phys.*, *3*, 1093–1100.

Mace, G. G., E. E. Clothiaux, and T. P. Ackerman (2001), The composite characteristics of cirrus clouds: Bulk properties revealed by one year of continuous cloud radar data, *J. Clim.*, *14*, 2185–2203.

Magee, N., A. M. Moyle, and D. Lamb (2006), Experimental determination of the deposition coefficient of small cirrus-like ice crystals near −50°C, *Geophys. Res. Lett.*, *33*, L17813, doi:10.1029/2006GL026665.

McFarquhar, G. M., J. Um, M. Freer, D. Baumgardner, G. L. Kok, and G. Mace (2007), Importance of small ice crystals to cirrus properties: Observations from the Tropical Warm Pool International Cloud Experiment (TWP-ICE), *Geophys. Res. Lett.*, *34*, L13803, doi:10.1029/2007GL029865.

Minikin, A., A. Petzold, J. Strom, R. Krejci, M. Seifert, P. van Velthoven, H. Schlayer, and U. Schumann (2003), Aircraft observations of the upper tropospheric fine particle aerosol in the Northern and Southern Hemispheres at mid latitudes, *Geophys. Res. Lett.*, *30*(10), 1503, doi:10.1029/2002GL016458.

Murphy, D. M., and T. Koop (2005), Review of the vapor presser of ice and supercooled water for atmospheric applications, *Q. J. R. Meteorol. Soc.*, *131*(608), 1539–1565.

Nelson, J. T., and M. B. Baker (1996), New theoretical framework for studies of vapor growth and sublimation of small ice crystals in the atmosphere, *J. Geophys. Res.*, *101*(D3), 7033–7047.

Ovarlez, J., J.-F. Gayet, K. Gierens, J. Strom, H. Ovarlez, F. Auriol, R. Busen, and U. Schumann (2002), Water vapour measurements inside cirrus clouds in Northern and Southern Hemispheres during INCA, *Geophys. Res. Lett.*, *29*(16), 1813, doi:10.1029/2001GL014440.

Peter, T., et al. (2003), Ultrathin Tropical Tropopause Clouds (UTTCs): I. Cloud morphology and occurrence, *Atmos. Chem. Phys.*, *3*, 1083–1091.

Peter, T., C. Marcolli, P. Spichtinger, T. Corti, M. B. Baker, and T. Koop (2006), When dry air is too humid, *Science*, *314*, 1399–1402.

Pruppacher, H. R., and J. D. Klett (1997), *Microphysics of Clouds and Precipitation*, 2nd ed., 954 pp., Kluwer Acad., Boston, Mass.

Rogers, D. C., P. J. DeMott, S. M. Kredenweis, and Y. Chen (1998), Measurements of ice nucleating aerosols during SUCCESS, *Geophys. Res. Lett.*, *25*(9), 1383–1386.

Seifert, M., J. Ström, R. Krejci, A. Minikin, A. Petzold, J.-F. Gayet, H. Schlager, H. Ziereis, U. Schumann, and J. Ovarlez (2004), Aerosol-cirrus interactions: A number based phenomenon at all?, *Atmos. Chem. Phys.*, *4*, 293–305.

Twomey, S. A. (1974), Pollution and the planetary albedo, *Atmos. Environ.*, *8*, 1251–1256.

J. E. Kay, Climate and Global Dynamics, National Center for Atmospheric Research, P.O. Box 3000, Boulder, CO 80307-3000, USA.

R. Wood, Department of Atmospheric Sciences, University of Washington, Seattle, WA 98195, USA.